Nontrivial Bloch oscillations in waveguide arrays with second-order coupling

Gang Wang,[1,*] Ji Ping Huang,[1] and Kin Wah Yu[2]

[1]*Department of Physics, State Key Laboratory of Surface Physics, and Key Laboratory of Micro and Nano Photonic Structures (Ministry of Education), Fudan University, Shanghai, China*

[2]*Department of Physics, The Chinese University of Hong Kong, Shatin, NT, Hong Kong, China*

**Corresponding author: 071019009@fudan.edu.cn*

Received January 4, 2010; revised April 24, 2010; accepted April 30, 2010; posted May 12, 2010 (Doc. ID 122227); published May 28, 2010

Under the influence of the next-nearest-neighbor interaction, we theoretically investigate the occurrence of Bloch oscillations in zigzag waveguide arrays. Because of the special topological configuration of the lattice itself, the second-order coupling (SOC) can be enhanced significantly and leads to the band alteration beyond the nearest-neighbor model, i.e., the offset of minimum value from the band edge. Contrary to the behavior in the vanishing SOC, the oscillation patterns exhibit new features, namely, a double turning-back occurs when the beam approaches the band edge. Our results can be applied to some ordered-lattice systems.

OCIS codes: 130.2790, 230.7380.

The coherent dynamics of waves in periodic lattices is a rich branch of scientific research because of its fundamental phenomena and applications [1,2]. One interesting example is Bloch oscillation (BO). So-called BO occurs when wave packets do not follow the direction of a driving force but instead perform an oscillatory motion. A considerable amount of BO activity has been studied in a variety of physical systems [3–6]. In all these diverse contexts, BO was investigated in lattices whose sites are reasonably assumed to be nearest-neighbor coupled. Nevertheless, in some typical situations, the long-range interaction appears as an intrinsic feature of the system that cannot be eliminated. For example, the next-nearest neighbors in polymer chains have remarkable relevance for energy transfer [7]. However, to the best of our knowledge, BO in ordered lattices with second-order coupling (SOC) has not yet been investigated. The reason is obvious: the strength of SOC is too small to observe its effect. In view of its importance, it is natural to ask how to engineer lattices to enhance SOC and, thus, how SOC affects the dynamics of waves, which have motivated our present study. As expected, we reveal some new features of BO's evolution, compared with the conventional behavior (see, for instance, [2]).

In this Letter, we show that waves propagating in systems with SOC can be *nontrivial* Bloch oscillations. For demonstration purposes, we investigate the evolution of light in waveguide arrays (one kind of accessible and widely used realization of the lattice model [8,9]). The extended interactions are introduced through a special topological arrangement of the single guide, leading to strong and observable SOC. The band structures are modified within the Brillouin zone, accordingly. As a result of this band alteration, the oscillation patterns present a double turning-back at the band edge. Correspondingly, the phase diagram shows nontriviality.

The optical lattice system under investigation is formed by a single-mode waveguide, as depicted schematically in Fig. 1 [10]. All waveguide elements are identical and equally spaced from each other. However, they are in a two-layer arrangement and the distance between the layers is close enough so as the modal fields supported by these waveguides overlap; as a result, cross talk takes place. Such a zigzag arrangement serves as a planar array with defined SOC [10–13]. The corresponding discrete evolution equation yields the band structure of the lattices, i.e., the dependence of the longitudinal wave vector component k_z on the transverse Bloch momentum k_x (normalized in π/d): $k_z = \beta_0 + 2\kappa_1 \cos(k_x) + 2\kappa_2 \times \cos(2k_x)$ [10–13]. Here β_0 represents the propagation constant of a waveguide. The dispersion relation is depicted in Fig. 1 for two different values of SOCs, namely $\Lambda = 0.0$ and 0.7. First, we would like to discuss the properties of the dispersion curve at the limit $\Lambda = 0$. In this case, the dispersion curve attains a maximum at $k_x = 0$. We can also notice that, at the edge of the Brillouin zone, i.e., $k_x = \pi/d$, the dispersion curve reaches a minimum. In other words, the dispersion relation is a monotonic function in the zone. However, as clearly seen from Fig. 1, the properties of the dispersion relation can be

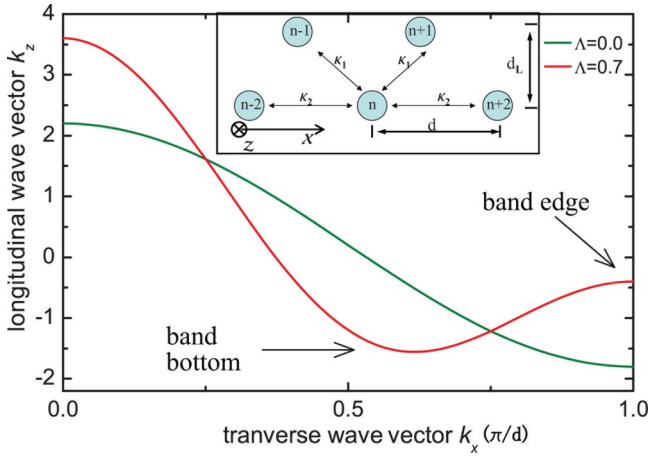

Fig. 1. (Color online) Band structures of waveguide arrays with (without) next-nearest-neighbors coupling. The inset gives the waveguide array. The zigzag arrangement is designed to enhance the SOC. Here x is defined as the transverse dimension and z as the propagation dimension. The distances between the guides and between the layers are denoted with d and d_L, respectively, and $\kappa_{1(2)}$ denotes the first (second)-order coupling resulting from the field overlap. The parameter $\Lambda = \kappa_2/\kappa_1$ is introduced to describe the ratio between second- and first-order coupling strength.

drastically altered for the SOC. It exhibits a nonmonotonic behavior compared to that with vanishing SOC. The minimum value is in the middle of the Brillouin zone instead of the band edge. Here, we show that it is the deviation of the dispersion minimum that plays the key role in changing the behavior of the BO.

To obtain the desired BO, we superimpose a linear potential across the array $\beta_n = n\sigma$. Here, the transverse potential acts as an analogue of external driving force **F** and is directly related to the refractive index change between the adjacent waveguides. This variation can be achieved by either electro- or thermo-optically changing the effective index of the waveguides [5,14,15] or by using a curved waveguide array [2].

In the problem involving light moving in lattices, we could set about solving the Schrödinger equation. However, it is well known that wave-packet solutions of the Schrödinger equation follow the same trajectories as classical particles, obeying the equations of motion derived from the Hamiltonian in the classical pictures (Erenfest theorem) [16,17]. Hence, to get an insight into the ray trajectories, let us analyze the quasi-classical pictures first. Figure 2 displays the depth-dependent band diagram under the gradation, and we can find the peculiarity of the band diagram to the SOC case. Clearly, the band region is separated into two sections. This originates from the offset of the dispersion minimum from the band edge, which causes the spectrum line of the minimum to appear on the lower side instead of that of the band edge. In the dynamic scenario, for the rays initially $n = 10$ and $k_x = 0$, the subsequent motion is governed by the Hamiltonian equations [17]. The linear potential causes the beam to gain transverse Bloch momentum and accelerates the momentum to drift through the reciprocal space from $k_x = 0$ to $2\pi/d$. At $z = z_B/2$ (z_B is BO's period), the ray touches the band edge, while transverse momentum reaches $k_x = \pi/d$. At this point, we have a Bragg reflection. However, during this propagation, one additional process appears to result from the aforementioned offset. That is, before encountering the band edge, the pulse is first reflected back by the bottom of the band; otherwise, it would be in the bandgap. After a cycle, the reformation of the light distribution occurs at the input position. This yields the full series of displacement. Hence, when light waves are incident on the system, waves are reflected at three turning points. These turning points include the band top, bottom, and edge. Apparently, the first two positions correspond to the bandgaps, while the reflection at the band edge is due to the Bragg resonance. This is quite different from the conventional behavior, of which two turning points are included, i.e., band top and edge.

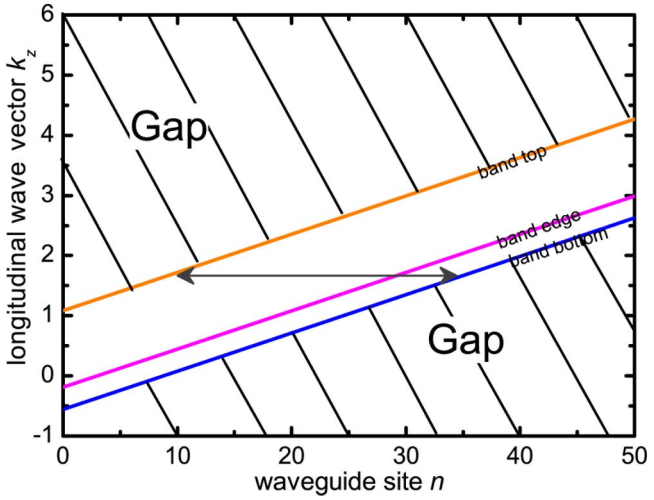

Fig. 2. (Color online) Band diagram of waveguide arrays superimposed; the linear potential $\sigma = 0.2$. Crossed areas correspond to the gaps, while the white areas indicate the band. Clearly, the band is separated into two sections by the band edge. Parameter: $\Lambda = 0.7$.

Let us move to the phase diagram. The trajectories of evolution in the phase space $(\langle n\rangle, \langle k_x\rangle)$, shown in Fig. 3, indicate that the phase diagram is enriched as compared with typical investigations [16]. The BO of SOC develops a waist-shaped track, whereas conventional BO corresponds to the other orbit. The cross point at $k_x = \pi/d$ of these orbits is directly related to the Bragg resonance of light, which is shared by both cases.

Let us now turn to a formal discussion beyond the quasiclassical analysis. The field evolution in the case of linear potential can be described by a modified discrete model as follows [8,9]:

$$-\imath\frac{da_n}{dz} = \sigma n a_n + \kappa_1(a_{n+1} + a_{n-1}) + \kappa_2(a_{n+2} + a_{n-2}).$$

Assume the Gaussian beam

$$W \propto \exp(-\frac{(n-n_0)^2}{W_0^2})\exp(\imath k_x d)$$

is initially centered at $n_0 = 10$ and carries phase difference $k_x d = 0$. In the vanishing SOC regime ($\kappa_2 = 0$), e.g., the investigations of [5,6,14], the well-known BO graph of light can be found in Fig. 4(a). Conversely, please note that in Fig. 4(b) the oscillation pattern of SOC differs from the conventional BO. Evidently, the pulse oscillates in the same transverse spatial range, and an additional process on the basis of the conventional BO, namely, double turning-back, appears. This is why we call it nontrivial BO. It is obvious that the offset plays a key role in the path back and forth. The effect of SOC on the oscillation patterns is even more pronounced when the ratio Λ increases.

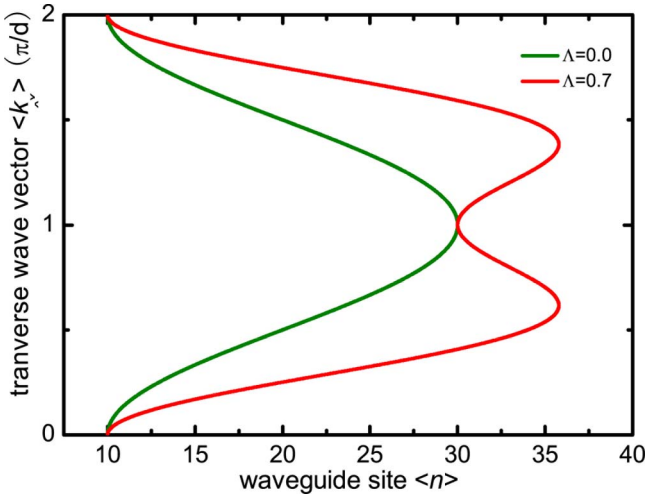

Fig. 3. (Color online) For the same linear potential $n\sigma$, the orbits $\langle n\rangle - \langle k_x\rangle$ in phase space for lattices with various SOCs.

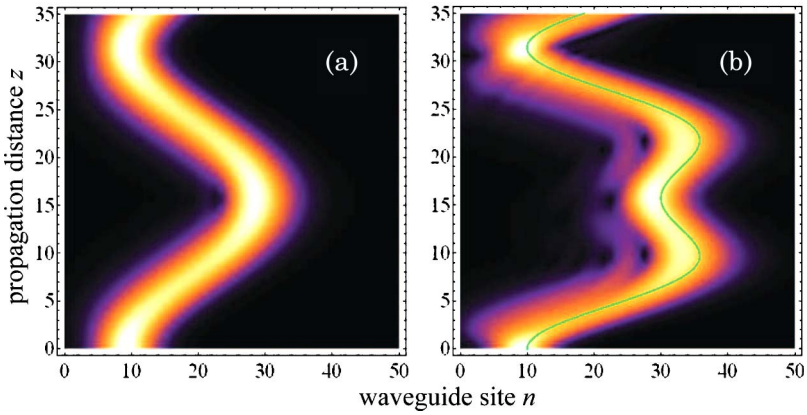

Fig. 4. (Color online) Evolution of the launched Gaussian beam. Compared with the typical BO [Fig. 4(a)], the dynamics with the SOC [Fig. 4(b)] clearly behaves in a different pattern. The solid curve is the dispersion relation of the homogeneous waveguide arrays, which is scaled by $1/\sigma$. Parameters: (a) $\Lambda = 0.0$, (b) $\Lambda = 0.7$.

By comparing Figs. 4(a) and 4(b), we can find some remarkable features. First, the periods of nontrivial and trivial BO are equal. We can look for the reason within the semiclassical pictures. In the reciprocal space, the beam will scan the Brillouin zone periodically, leading to the estimate of the oscillation period $T_B = 2\pi/F$. Apparently, the BO period is only relevant to the tilting of the band. On the other hand, as observed in Fig. 4, the transverse spatial extension of oscillation is dependent on the SOC. Within a half of the oscillation period, the beam is displaced by $L = \Delta/F$, where Δ denotes the width of the band. Because of the introduction of SOC, the bandwidth of zigzag arrays is broader than that of the chain case, which accordingly causes a larger transverse range.

Herein are some comments. It is a known fact that BO almost directly reflects the band structure [18]. Figure 4(b) displays that the evolution pattern reproduces the shape of the band of our SOC model. This provides a good example to demonstrate the general validity of the relationship between BO and the corresponding band structure [17]. However, BO in an optical lattice is only a visual demonstration; it is not precise because the spatial path of BO has a width of field distribution, while each band in the spectrum is a curve. The curve does not follow the mean trajectory of BO exactly. Meanwhile, an as-yet undetermined integration constant needs to be confirmed during the mapping of the band structure by BO.

The case of higher-order couplings is a simple extension of our study and similar results can be obtained. We do not discuss it here. Some applications derived from our study are mentioned. Our proposal can be applied in the field of terahertz generation from BO. Electrons performing BOs in an energy band of a dc-biased semiconductor superlattice can generate THz fields [3]. Apparently, the double turning-back will lead to higher harmonics besides the fundamental BO frequency. Also, it can create new applications for all-optical routing, e.g., beam steering [15] and imaging [19].

To conclude, we have shown how the long-range interactions affect the BO. A double turning-back occurs when the beam approaches the band edge because of the derivation of the band bottom from the edge. The results can be extended to other periodic systems, e.g., cold atoms in optical lattices, because of the similar dynamic scheme owing to the periodicity.

G. Wang is indebted to Shaoyu Yin for stimulating discussions. This work is supported by the National Natural Science Foundation of China (NSFC), grant 10874025, and the Chinese National Key Basic Research Special Fund (CNKBRSF), grant 2006CB921706. K. W. Yu acknowledges support from the Research Grants Council.

References and Notes

1. O. Morsch and M. Oberthaler, Rev. Mod. Phys. **78**, 179 (2006).
2. S. Longhi, Laser Photon. Rev. **3**, 243 (2009), and references therein.
3. C. Waschke, H. G. Roskos, R. Schwedler, K. Leo, H. Kurz, and K. Köhler, Phys. Rev. Lett. **70**, 3319 (1993).
4. M. B. Dahan, E. Peik, J. Reichel, Y. Castin, and C. Salomon, Phys. Rev. Lett. **76**, 4508 (1996).
5. T. Pertsch, P. Dannberg, W. Elflein, A. Bräuer, and F. Lederer, Phys. Rev. Lett. **83**, 4752 (1999).
6. R. Morandotti, U. Peschel, J. S. Aitchison, H. S. Eisenberg, and Y. Silberberg, Phys. Rev. Lett. **83**, 4756 (1999).
7. D. Hennig, Eur. Phys. J. B **20**, 419 (2001).
8. D. N. Christodoulides, F. Lederer, and Y. Silberberg, Nature **424**, 817 (2003).
9. F. Lederer, G. I. Stegeman, D. N. Christodoulides, G. Assanto, M. Segev, and Y. Silberberg, Phys. Rep. **463**, 1 (2008).
10. N. Efremidis and D. Christodoulides, Phys. Rev. E **65**, 056607 (2002).
11. F. Dreisow, A. Szameit, M. Heinrich, T. Pertsch, S. Nolte, and A. Tünnermann, Opt. Lett. **33**, 2689 (2008).
12. A. Szameit, R. Keil, F. Dreisow, M. Heinrich, T. Pertsch, S. Nolte, and A. Tünnermann, Opt. Lett. **34**, 2838 (2009).
13. A. Szameit, T. Pertsch, S. Nolte, A. Tünnermann, and F. Lederer, Phys. Rev. A **77**, 043804 (2008).
14. U. Peschel, T. Pertsch, and F. Lederer, Opt. Lett. **23**, 1701 (1998).
15. T. Pertsch, T. Zentgraf, U. Peschel, A. Bräuer, and F. Lederer, Appl. Phys. Lett. **80**, 3247 (2002).
16. S. Longhi, Phys. Rev. B **76**, 195117 (2007).
17. From the Hamiltonian $H = \sigma x + 2\kappa_1 \cos(k_x) + 2\kappa_2 \cos(2k_x)$ [16], the motion equations are given: $\mathrm{d}x/\mathrm{d}z = \mathrm{d}H/\mathrm{d}k_x$, $\mathrm{d}k_x/\mathrm{d}z = -\mathrm{d}H/\mathrm{d}x$. With appropriate initial conditions, solutions take the form $k_x = \sigma z$, $x = x_0 - (2/\sigma)(\kappa_1 + \kappa_2) + (2\kappa_1/\sigma)\cos(\sigma z) + (2\kappa_2/\sigma)\cos(2\sigma z)$. The BO path directly reflects the corresponding dispersion relation magnified by $1/\sigma$. The Hamiltonian optics offer a good approximation of the field evolution.
18. A. Fratalocchi and G. Assanto, Opt. Lett. **31**, 3351 (2006).
19. S. Longhi, Opt. Lett. **33**, 473 (2008).